

PAPER • OPEN ACCESS

## Hierarchical optimization approaches in designing surface hardening induction systems

To cite this article: M. Baldan *et al* 2018 *IOP Conf. Ser.: Mater. Sci. Eng.* **424** 012067

View the [article online](#) for updates and enhancements.



**IOP | ebooks™**

Bringing you innovative digital publishing with leading voices to create your essential collection of books in STEM research.

Start exploring the collection - download the first chapter of every title for free.

## Hierarchical optimization approaches in designing surface hardening induction systems

M. Baldan<sup>1</sup>, A. Nikanorov<sup>1,2</sup>, B. Nacke<sup>1,2</sup>

<sup>1</sup>Institute of Electrotechnology, Leibniz University Hannover, Wilhelm-Busch-Str. 4, 30167 Hannover, Germany

<sup>2</sup>Department of Electrotechnology and Converter Engineering, St. Petersburg Electrotechnical University, Prof. Popov Str. 5, St. Petersburg, Russia

Marco Baldan: baldan@etp.uni-hannover.de

### Abstract

Induction surface hardening is a quite traditional and well-known process in which a metal part is induction-heated and then quenched. The quenched metal undergoes a martensitic transformation, increasing the hardness and stiffness of the part. The design of a surface hardening system is a challenging task. This paper describes an approach to divide a full problem into simpler ones and to optimize the electrical regime. We compare the effectiveness of using a single-objective rather than a multi-objective optimization approach.

**Key words:** hierarchical optimization, multi-objective optimization, induction hardening.

### Introduction

The design of induction hardening systems involves defining both the electrical regime and geometry of the induction coil. This implies a considerable number of degrees of freedom, which must be set in order to reach a given goal. In the last decades, the use of numerical simulations has been a key element in designing induction systems. Especially in the case of complex geometry work-pieces, using only one numerical model for establishing the whole degrees of freedom set can be extremely time consuming. In order to overcome this issue, the full problem may be divided into simpler ones [1-2].

Optimization plays a key role in designing induction heating systems [3]. Some optimization models dealing with induction hardening by means of numerical simulation [4] or experiments [5-9] can be found in the literature. Naar et al. [4] optimized frequency and current density to achieve a temperature rise in a fixed time. Qin et al. [5] presented a response surface method (RSM) for studying and optimizing the effect of five process parameters (feed velocity, input power, gap, curvature and flow rate) on temperature, microstructure, microhardness, and phase transformation geometry in a spot continual induction hardening process. Kayacan et al. [9] applied a fuzzy approach to study the influence of coil air-gap, material diameter, cooling time, power, and frequency on the hardening depth and heating time.

In this paper, we intend to present a hierarchical approach for fully optimizing a surface hardening induction system. Starting from a complex geometry work-piece, we determinate the heating time, frequency, and current that optimally provide the desired hardening depth. The first part of the article describes the attempt to optimize the electrical regime by coupling a one-dimensional model with a multi-objective optimization algorithm. The second part investigates the use of a single-objective approach for optimizing, separately, frequency and heating time.

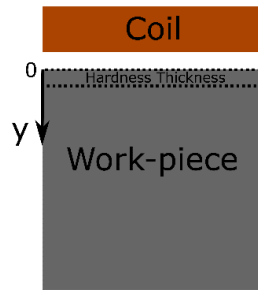
### 1D Numerical model

Numerical simulations were carried out with the commercial package ANSYS®. The one-dimensional numerical model has a planar shape and consists of a square work-piece and a massive copper coil (Fig. 1). Because the model is one-dimensional, every quantity changes only in the transversal direction ( $y$  in Fig. 1). The heating process has been simulated through a harmonic electromagnetic analysis coupled with a transient thermal one. Both electrical and thermal material properties are temperature-dependent. In order to obtain reliable results in induction hardening simulation, the dependency of the magnetic permeability on the magnetic field strength must be taken into account [10]:

$$\mu = 1 + (2.41^{14.73 - \ln H} - 1)(1 - (T/T_C)^2) \quad (1)$$

Where  $\mu$  is the relative magnetic permeability,  $H$  the magnetic field strength [A/m],  $T$  the temperature [°C], and  $T_C$  the Curie temperature. The quenching phase, which is supposed to start immediately after the heating phase, has been simulated with an equivalent temperature dependent heat transfer coefficient (Fig. 2) [11]. Quenching time is 60 seconds, long enough to cool down the work-piece under 100 °C. Considering that the present work focuses more on the heating stage, it should be noted that neither the flow rate nor the quenching time is an object of our optimization. From the temperature history of each node of the mesh, making use of [12], the final distribution of martensite has been calculated. In this model, the content of martensite in one point is dependent on three aspects: whether the AC<sub>3</sub> temperature has been reached or not, the average cooling rate, and the temperature after the quenching phase. If necessary, the hardness





distribution is easily obtainable from the microstructure calculation

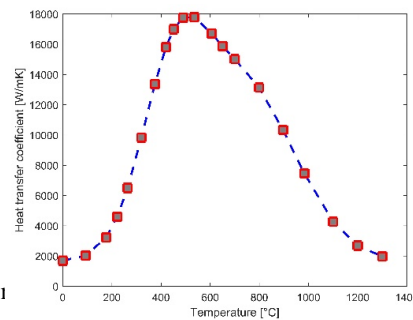


Fig. 2: Dependency of the heat transfer coefficient on temperature for simulating the quenching phase.

Fig. 1: Geometry of the 1D model. The coil is a massive piece of copper.

**Multi-objective optimization using the 1D model**

A great benefit of the one-dimensional model is its non-dependence on the work-piece geometry. Once the 1D model has been coupled with an optimization algorithm, it establishes a tool able to estimate the optimal heating time and frequency. The current is a parameter of optimization too. However, the optimal current value cannot be directly used in the next hierarchical steps because it must be adapted to the surface power that is needed in order to heat the work-piece. At the same time, results of 1D model enable us to estimate the necessary power density and therefore the installation power needed.

The parameters that affect results of optimization are the steel grade, the cooling medium, the cooling time and rate, plus, of course, the hardening depth. The carbon steel C56 is considered in this study. The cooling medium is water with an estimated quenching effect visible in Fig. 2. Results of optimization are thus a function only of the hardening depth.

For the first investigations, we decided to simplify the numerical model and to consider only the heating phase. In doing so, we identify the hardening depth with the part of the work-piece that has been heated up over the  $AC_3$  temperature, i.e. over 850°C. In other words, for example in the case of 3 mm hardening depth, a temperature of 850 °C has to be achieved 3 mm distant from the surface. The multi-objective optimization algorithm AMALGAM\* [13] has been employed for the analysis. A three dimensional vector  $x$  of investigated variables (heating time, frequency and current) has been defined. Our first attempt focused on the trade-off between three conflicting functions, i.e. surface temperature  $f_1(x)$ , energy consumption  $f_2(x)$  and heating accuracy  $f_3(x)$ . Heating accuracy in this case means how the evaluated temperature in the hardening depth differs from  $AC_3$ . It turned out that such approach is ineffective in our case, since we are interested only in the part of the Pareto front in which  $f_3(x)$  trends to zero.

The next step we took was to modify the optimization algorithm. Similar to [14], a double loop was introduced (Fig. 3). AMALGAM\* was used in the “external loop” where the vector variable is now two dimensional (heating time and frequency) and two objective functions ( $f_1$  and  $f_2$ ) are considered. The “internal loop” is simply intended to find the right current that zeroes  $f_3$  and it is based on a golden section search and a parabolic interpolation. In fact, given a frequency and a heating time, there is only one value of current that able to reach the  $AC_3$  temperature in the hardening depth. As a result, each point of the obtained Pareto front is a potential solution. Despite the considerable computational time, this approach is preferable.

The following presents the results obtained with 1 and 3 mm as hardening depth. Table 1 summarizes the search ranges of the variables.

	1 mm Hardening depth	3 mm Hardening depth
Heating time [s]	3 - 20	3 -20
Frequency [kHz]	10-100	1-20

Table 1: Variable ranges

Fig. 4 shows respective 1 and 3 mm Pareto fronts after 15 generations using a population of 25 individuals. Figs. 5a and 5b indicate instead the “image” of the Pareto front, i.e. the values that the variables assume, for the 1 mm case. As expected, the point with minimum surface temperature is characterized by the maximum time and the minimum frequency. But

surprisingly, the front can be divided into two parts. In the “left” part all the points assume the minimum range frequency, whereas in the “right” one the heating time is always at minimum. From these results we can conclude that the frequency plays a minor role compared to the heating time in terms of energy consumption. Further simulations with different time ranges and hardening depths showed analogous results. In other words, in this approach, the choice of the variable ranges directly affects the obtained Pareto front. Therefore, we adopted a new strategy.

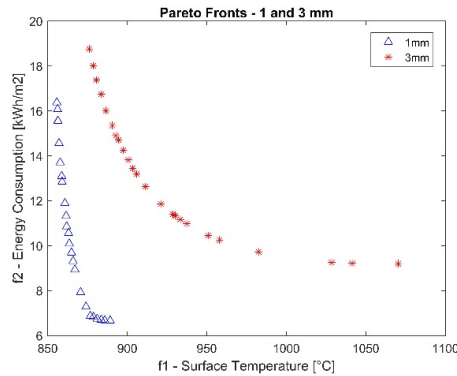


Fig. 4: Pareto fronts with 1 and 3 mm hardness depth.

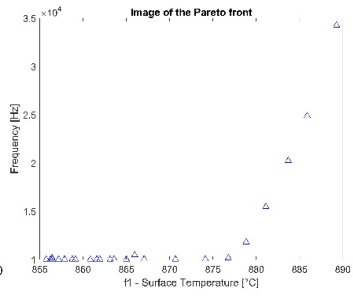


Fig. 5a: Frequency assumed by the points in the Pareto front.

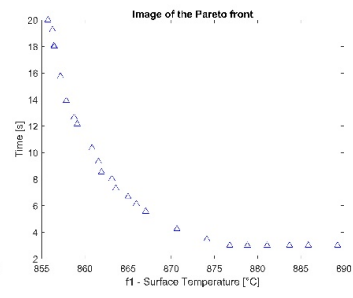


Fig. 5b: Heating time of the non-dominated solutions.

**Single-objective optimization of the 1D model**

As described above, in the Pareto front, the point with the lowest energy consumption is the point with the optimal frequency and minimum time. It is relevant to underline that no constraints on the maximum available power are taken into account. This means that a multi-objective optimization approach is here overabundant. Considering a typical heating time, the optimal frequency can be evaluated considering the energy consumption as a unique objective function. Of course, even in this case, a “double loop” approach is required and for each frequency, the current value must be corrected. Table 2 shows results of optimal frequency for several hardening thicknesses evaluated at different heating times.

	Heating time	3 s	6 s	12 s	Reference
Hardening depth	1 mm	42.4 kHz	not found	not found	<b>60 kHz</b>
	3 mm	9.6 kHz	8.5 kHz	6.5 kHz	<b>6.67 kHz</b>
	5 mm	3.0 kHz	3.2 kHz	3.0 kHz	<b>2.4 kHz</b>
	8 mm	1.04 kHz	1.09 kHz	1.03 kHz	<b>0.94 kHz</b>

Table 2: Optimal frequencies for different heating times and hardening depths.

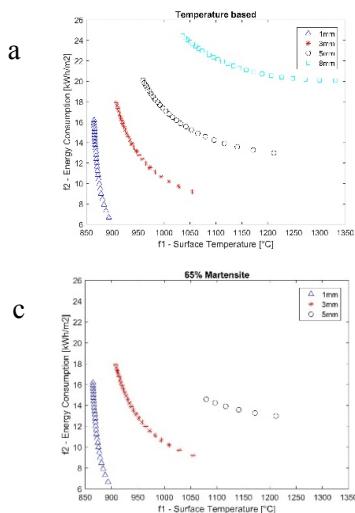


Fig. 6a: Temperature based trade-off with 1, 3, 5, 8 mm.

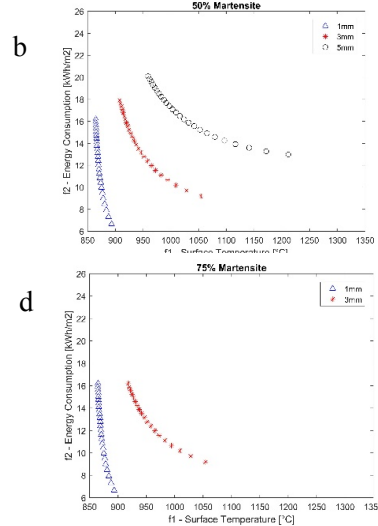


Fig. 6b,c,d: Microstructure base trade-off.

In the 1 mm hardening depth case, the energy consumption shows a clear minimum only if the heating time is short (3 s). The heating time partly influences the optimal frequency, especially in the case of 3 mm thickness. The values found are in good agreement with the literature [15] (see "Reference" in Table 2).

#### **Trade-off between energy consumption and surface temperature**

Once the frequency has been chosen, we studied how the heating time influences the energy consumption and surface temperature. The heating time ranges from 3 to 20 s. Fig. 6a shows results based only on the heating stage. Especially with small hardening depths, a heating time reduction could dramatically cut the energy consumption. Results in Figs. 6b, 6c and 6d also involve the microstructure calculation. Fig. 6b illustrates the energy-temperature trade-off in the case where the minimum content of martensite in the hardening depth is 50 %. It is not possible to reach such result in the case of 8 mm thickness. Figs. 6c and 6d summarize the trends with 65 % and 75 % minimum martensite content respectively. In order to get 5 mm thickness with a minimum martensite content of 65 %, the heating time must be shorter than 6.5 s (Fig. 6c). With 3 mm hardening depth instead, the heating time cannot be longer than 16 s in order to achieve a 75 % martensite content (Fig. 6d).

#### **Conclusions**

We showed how to optimize the frequency and the heating time in a surface induction heating application. We proved that only for small hardening depths, i.e. 1 mm, it is possible to optimize the process just on the basis of the temperature distribution. This is admissible with medium hardening depths (3 mm) too, as long as the heating time is relatively short (shorter than 16 s in our case study). With bigger thicknesses (5 mm or more) the phase change simulation is a requirement for getting reliable results.

#### **References**

1. T. Zedler, Numerische Modellierung, Analyse und Design von induktiven Systemen für das Randschichthärten komplexer Werkstückgeometrien, PhD Thesis, Sierke Verlag (2010)
2. D. Schlesselmann, Methoden zur numerischen Berechnung, Analyse und Auslegung induktiver Randschichthärteprozesse unter Berücksichtigung von magnetischen Sättigungseffekten, PhD Thesis, PZH Verlag (2016)
3. Yu. Pleshivtseva, E. Rapoport, B. Nacke, A. Nikanorov, P. Di Barba, M. Forzan, S. Lupi, E. Sieni, Design concepts of induction mass heating technology based on multiple-criteria optimization, *COMPEL: The International Journal for Computation and Mathematics in Electrical and Electronic Engineering*, 36,2 (2017), 386-400
4. R. Naar, F. Bay, Numerical optimization for induction heat treatment processes, *Applied Mathematical Modeling*, 37 (2013), 2074-2085
5. X. Qin, K. Gao, Z. Zhu, X. Chen, Z. Wang, Prediction and optimization of phase transformation region after spot continual induction hardening process using response surface model, *JMEPEG*, 26 (2017), 4578-4594
6. M. Onan, H.I. Unal, K. Baynal, F. Katre, Optimization of induction hardened AISI 1040 steel by experimental design method and material characterization analysis, *Proceedings of the ASME International Mechanical Engineering Congress & Exposition*, (2012), November 9-15, 2012, Huston, Texas USA
7. M. K. Misra, B. Bhattacharya, O. Singh, A. Chatterjee, Multi response optimization of induction hardening process – a new approach, *Proceedings of the 3<sup>rd</sup> International Conference on Advances in Control and Optimization if Dynamical Systems*, (2014), March 13-15, 2014, Kanpur, India
8. A. Kohli, H. Singh, Optimization of processing parameters in induction hardening using response surface methodology, *Sadhana*, 36, 2 (2011), 141-152
9. M. C. Kayacan, O. Colak, A fuzzy approach for induction hardening parameters selection, *Material and Design*, 25 (2004), 155-161
10. U. Lüdtke, Numerische Simulation gekoppelter Felder in der Elektroprozessstechnik, Habilitation, (2013)
11. A. D. Demichev, Surface hardening by induction method, Politechnika, Leningrad, 1991
12. D. Schlesselmann, A. Nikanorov, B. Nacke, S. Galunin, M. Schön, Z. Yu, Numerical calculation and comparison of profiles and martensite microstructure in induction surface hardening processes, *Proceedings of HES-13*, (2013), Padova, Italy, 127-134
13. M. Baldan, T. Steinberg, E. Baake, Self-adaptive multimethod optimization search applied to a tailored heating forging process, *Proceedings of Modelling for material processing*, (2017), September 21-22, 2017, Riga, 191-200
14. S. Galunin, Automatic optimization in designing of induction heaters based on numerical techniques, *Proceedings of XVIII International UIE-Congress*, (2017), June 6-9, 2017, Hannover, Germany, 385-390
15. A. Sluhotsky, C. Ryskin, Inductors for the induction heating, *Energia*, Leningrad, 1974